Oscillatory Activity in Neocortical Networks during Tactile Discrimination near the Limit of Spatial Acuity – Supporting Information

Bhim M Adhikari, K Sathian, Charles M Epstein, Bidhan Lamichhane, Mukesh Dhamala*

*Corresponding author with complete address:

Department of Physics and Astronomy, Georgia State University

29 Peachtree Center Ave., Science Annex, Rm 456

Atlanta, GA, 30303. Phone: 404-413-6043, E-mail: mdhamala@gsu.edu

I. Source dipoles and oscillatory activities

The average ERPs for correct responses were used in an MNE approach to reconstruct the inverse EEG solutions (source dipoles). Table S1 includes the information related to the locations, orientations and activation times of dipoles. Table S2 lists the information associated with the oscillatory power differences between later (140-210 ms) and earlier (30-140 ms) periods during correct responses. Table S3 lists similar information for net causal flow from nodes.

Table S1: The anatomical location, dipole orientation (components) and activation timeframes of localized sources obtained for correctly perceived stimuli using the minimum-norm estimate (MNE) approach.

Regions	Talairach coordinates (mm) x y z	Dipole orientation (components) x y z	Activation time (ms)
Primary somatosensory cortex (SI)	-43.1 -23.4 59.6	0.6 0.2 0.8	40 - 50
Lateral occipital complex (LOC)	51.6 -57.3 -9.1	-0.6 -0.4 0.6	118 - 132
Posterior intraparietal sulcus (pIPS)	21.9 -44.6 66.4	-0.5 0.6 0.7	150 - 170
Dorsolateral prefrontal cortex (dlPFC)	-23.5 24.5 52.4	-0.3 -0.5 0.8	160 - 210

Table S2: The significance level (p-value and corresponding t - value in parentheses, marked in boldface) for spectral power differences between later (140-210 ms) and earlier (30-140 ms) periods during correct responses (obtained from paired t-tests).

Regions	beta band (12 - 30 Hz)	gamma band (30 - 100 Hz)
Primary somatosensory cortex (SI)	**1.86×10^{-4} (-5.83)**	**6.3×10^{-4} (-5.42)**
Lateral occipital complex (LOC)	0.14 (1.61)	0.08 (-1.95)
Posterior intraparietal sulcus (pIPS)	**1.17×10^{-4} (-6.95)**	**5.5×10^{-3} (3.77)**
Dorsolateral prefrontal cortex (dlPFC)	**3.49×10^{-4} (-5.93)**	**4.0×10^{-4} (5.80)**

Table S3: The significance level (p-value and corresponding t-value in parentheses, marked in boldface) for net causal inflow differences between later (140-210 ms) and earlier (30-140 ms) periods of correct responses (obtained from paired t-tests).

Regions	beta band (12 - 30 Hz)	gamma band (30 - 100 Hz)
Primary somatosensory cortex (SI)	0.037 (2.24)	0.514 (-0.66)
Lateral occipital complex (LOC)	**6.01×10^{-4} (4.07)**	0.085 (1.81)
Posterior intraparietal sulcus (pIPS)	**2.85×10^{-4} (-4.39)**	**0.001 (3.77)**
Dorsolateral prefrontal cortex (dlPFC)	**2.23×10^{-4} (4.49)**	**0.009 (-2.89)**

II. Power, coherence and causality spectra

From the ensemble averages-removed single source trials for the correct responses, spectral quantities (power, coherence and Granger causality spectra) associated with nodes (L SI, R LOC, R pIPS and L dlPFC) and their networks were computed for all participants. Figure S1 shows some of the results from one participant before separating frequency band-specific activities for further analyses. There are two spectral peaks, one at around 15 Hz and

the other at around 80 Hz in the power, coherence and Granger causality spectra. To see whether trial-to-trial variability has any effect on the spectra, we removed ensemble averages from single trials by using the ASEO method (Xu et al., 2009) and computed these spectral quantities. Although the magnitude of these quantities decreased in the ASEO-treated data, the results did not change significantly. Figure S2 shows power and some of the Granger causality spectra obtained after using the ASEO method.

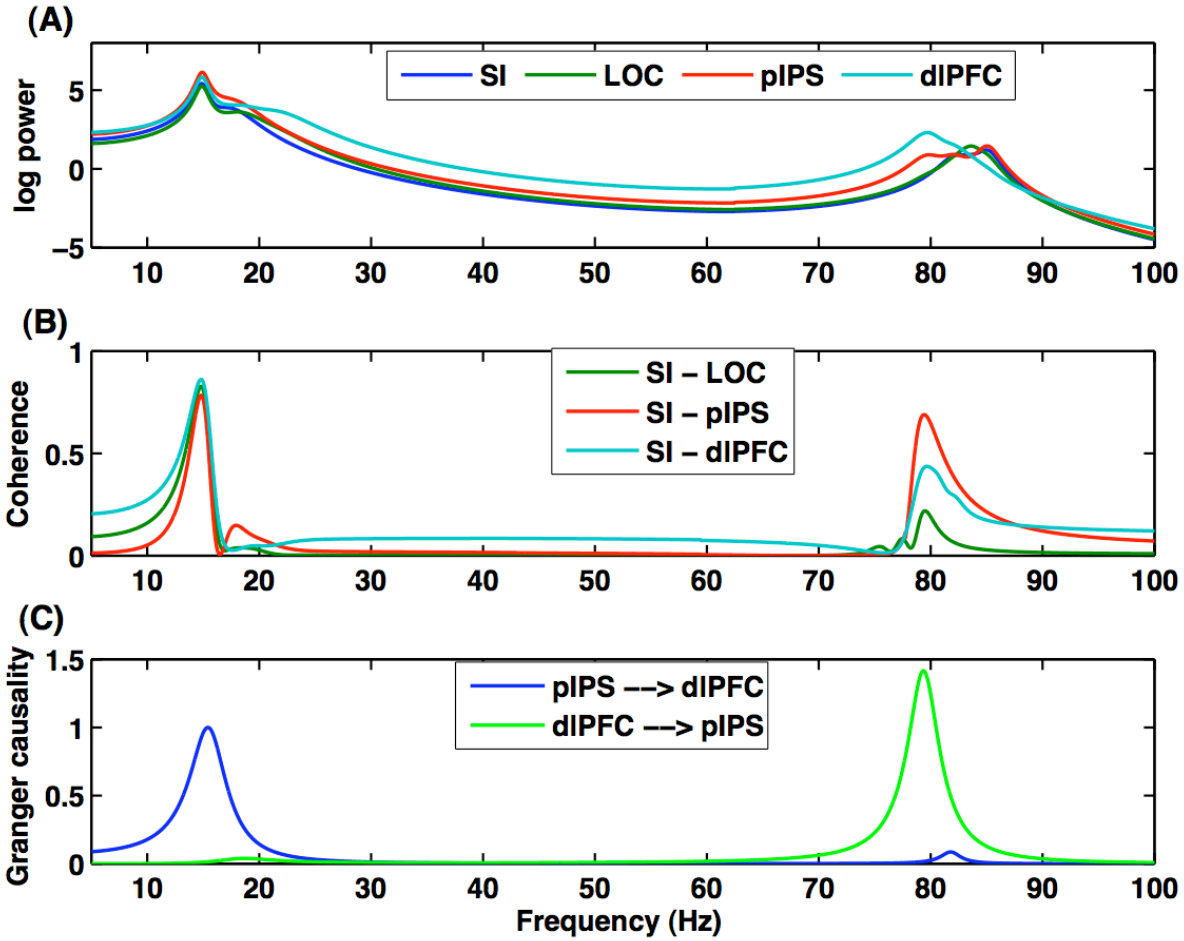

Figure S1. *Power spectra (A), coherence spectra (B) and Granger causality spectra (C) from a participant while performing a tactile discrimination task and providing the correct response.*

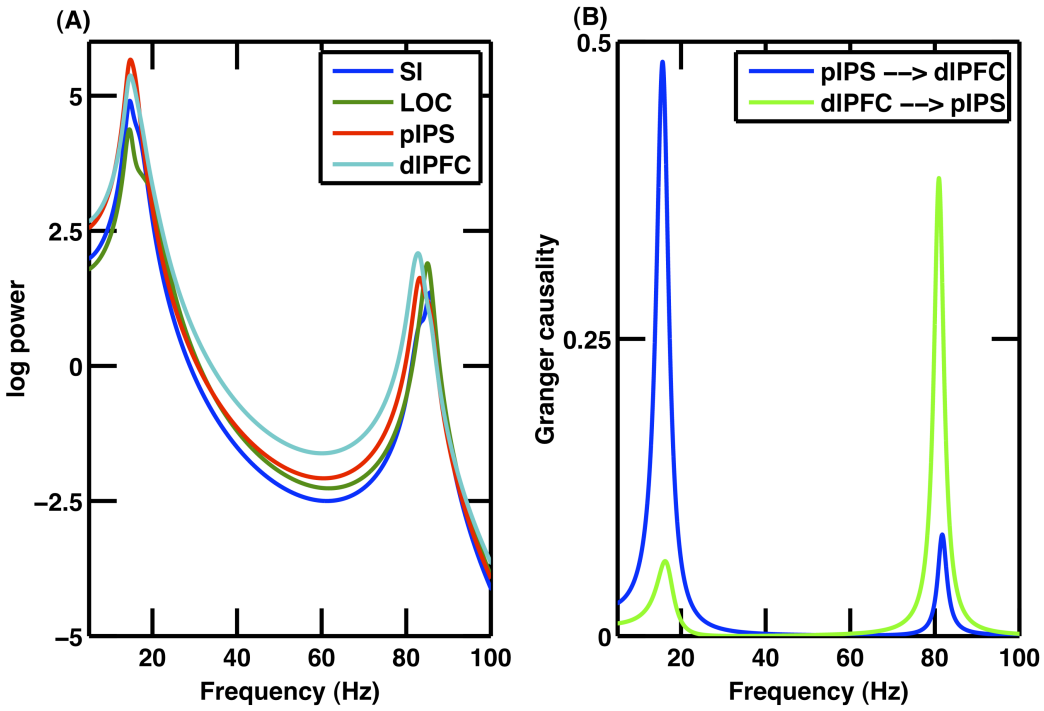

Figure S2: *Power spectra from all four nodes (A), and Granger causality spectra (B) from a pair of nodes (pIPS and dlPFC). These spectral measures were calculated from the single trial source waveforms after removing ensemble averages with the ASEO method. The Granger causality spectral peaks, though reduced in magnitudes, remain significant at ~15 Hz in beta and ~80 Hz in gamma frequency bands as in the traditional method.*

III. Dominant causal influences: feedforward, feedback or both?

To determine whether there was asymmetry between feedback and feedforward directed connectivity during tactile perceptual decision-making; we performed pairwise tests for the Granger causality values between feedforward and feedback connections in each participant in the post-stimulus period (30 to 210 ms). The net direction of interaction in the beta band network turned out to be feedforward ($p < 0.05$), whereas in the gamma band, it was found that there was no dominant feedforward or feedback interaction ($p < 0.05$) [Figure S3 (A-B)].

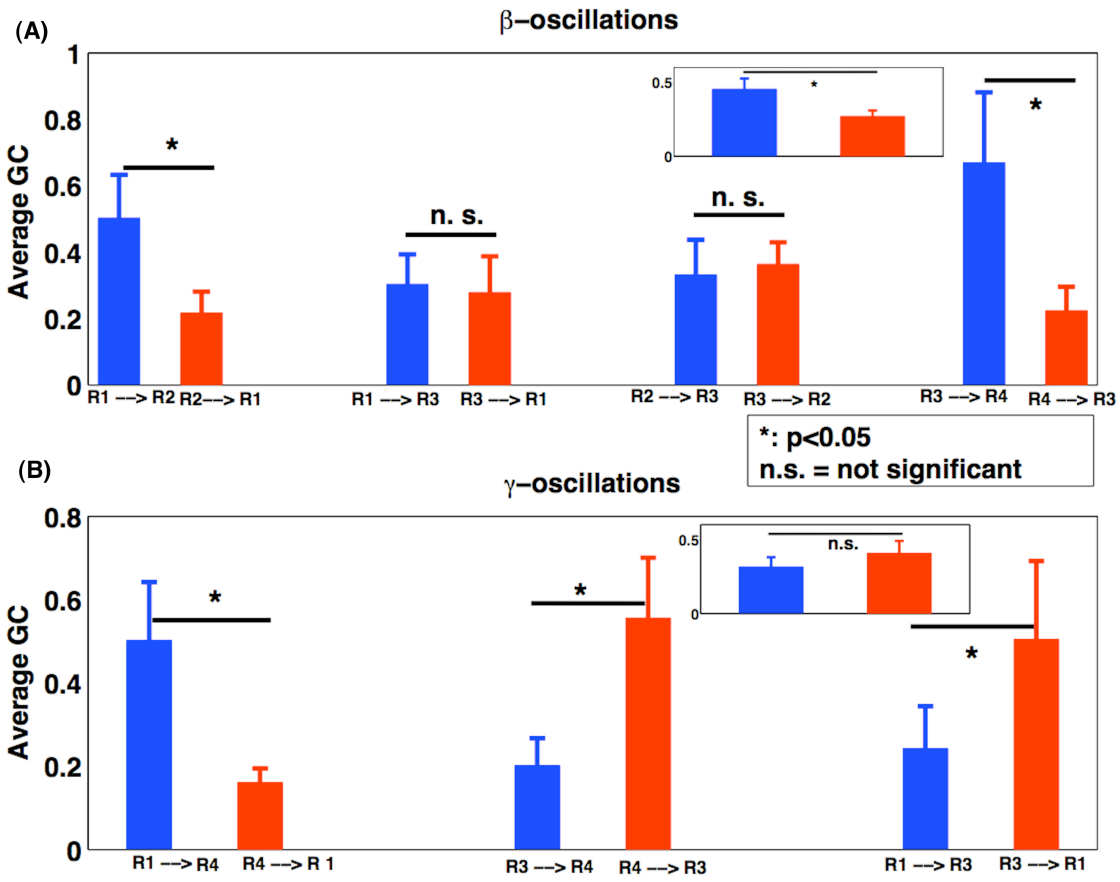

Figure S3*: Post-stimulus symmetrical and asymmetrical network activity in the beta band (A) and the gamma band band (B). Here, R1= L SI, R2 = R LOC, R3 = R pIPS and R4 = L dlPFC. Inset in (A) shows the overall feedforward interaction (blue) is significantly greater than the feedback interaction (red) in the beta band. The inset in (B) shows that there was no dominance of feedforward over feedback interactions, or the other way around; it was rather a recurrent loop for interaction (from SI to dlPFC, then to pIPS and to SI). Here, * indicates the significance of p< 0.05 and n.s. means not significant.*

Beta band network activity [Fig. S3 (A)]: Bidirectional interactions (feedback and feedforward) between SI and pIPS and between LOC and pIPS did not differ significantly. However, the feedforward interaction from SI to LOC was significantly stronger than the feedback interaction from LOC to SI. Also, the feedforward network interaction from pIPS to

dlPFC differed significantly compared to the feedback network interaction from dlPFC to pIPS. As shown in the inset [Fig. S3 (A)], the overall feedforward network interaction was significantly different from the feedback network interaction.

Gamma band network activity [Fig. S3 (B)]: The direction of interactions from SI to dlPFC, dlPFC to pIPS, pIPS to SI differed significantly from dlPFC to SI, pIPS to dlPFC, SI to pIPS respectively [Fig. S3 (B)]. The overall network interaction forming a recurrent loop (from dlPFC to pIPS, then to SI and then to dlPFC) was not significantly different from that of forming a recurrent loop the opposite direction (from dlPFC to SI, then to pIPS and then to dlPFC [inset Fig. S3 (B)].

IV. Absence of organized feedforward or feedback network activity in the prestimulus durations

In order to confirm that the observed network interaction patterns and Granger-causality based interactions could not be observed in the absence of task performance, we analyzed the data from the prestimulus period (-100 to 0 ms), computing Granger causality in the beta and gamma bands. As shown in Figure S4 (A-B), there was an absence of organized feedforward or feedback network activity in the prestimulus durations in both beta and gamma bands.

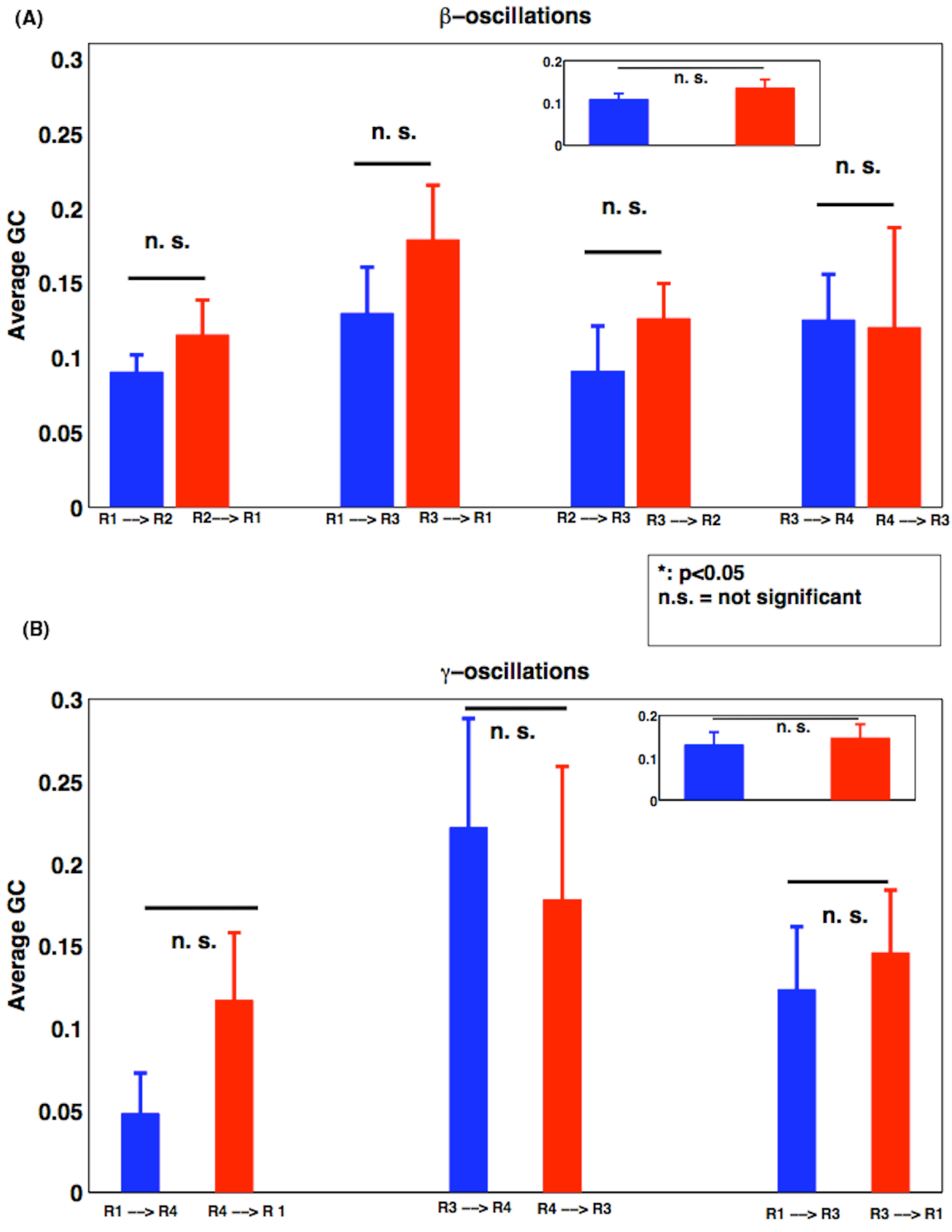

Figure S4*: Prestimulus network in beta band (A) and gamma band (B). Abbreviations and colors as in Figure S1. Neither the feedforward and feedback network interactions nor the*

overall feedforward and feedback direction of interactions (insets) were significantly different during the prestimulus period. R1, R2, R3, and R4 as in Fig. S3.

V. Network activity is not a result of residual volume conduction in the source signals

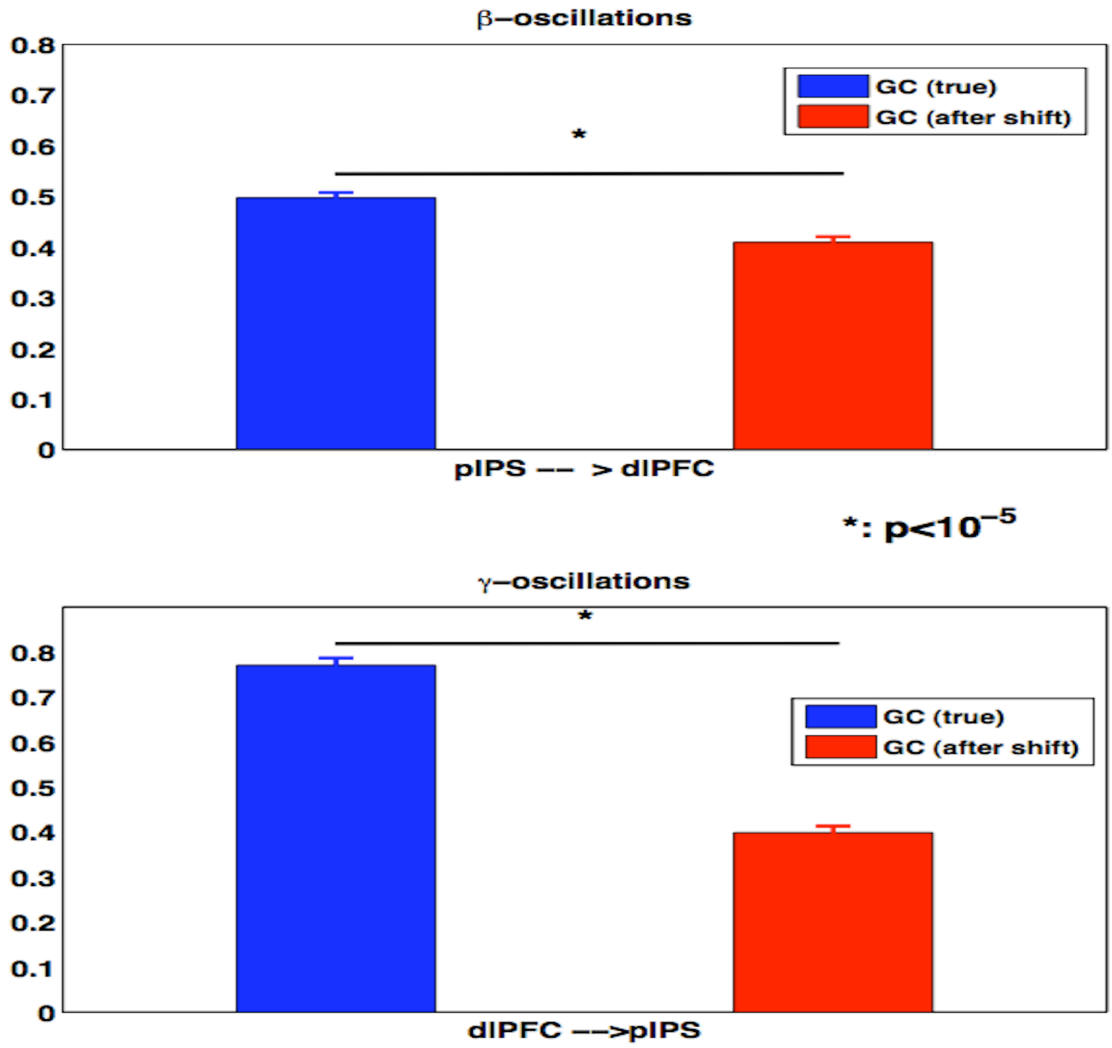

Figure S5*: Effect of any residual volume conduction in the source signals: true Granger causality (blue) and that obtained after shifting the time points (red). Here time points were shifted by, t =1, 2, 3, 4, 5 points to generate surrogate time series and to test the hypothesis that Granger causality would strengthen by time-shifting the driven signals if volume conduction effects were present in the data.*

We used the procedure of time-shifting driven signals used in previous studies (Faes et al., 2013; Lindner et al., 2011) to evaluate potential effects of residual volume conduction in the reconstructed source signals, to rule out the possibility that Granger causality patterns had anything to do with volume conduction. The comparison between the maximum Granger causality values of the original time series and the distribution of its values obtained for a set of 50 time-shifted surrogates for correct trials associated with two nodes (pIPS and dlPFC) showed the directed causal influences were not the result of volume conduction.

VI. Time-frequency maps of power, coherence and causality spectra

We performed time-frequency analyses separately for both beta and gamma band oscillations and examined the power spectra, coherence spectra and Granger causality spectra to better assess the spectral specificity and temporal evolution of neuronal effects for the duration of -100 to 600 ms.

Beta-oscillations: All the activation nodes demonstrated peak power at around 15 Hz, with pIPS showing the highest value and LOC, the lowest [Fig. S6 (1st column)]. Fig. S6 (2nd column) shows the coherence spectra peaking at around 15 Hz. From pairwise Granger causality spectra (3rd and 4th columns of Fig. S6), the interactions between SI and LOC, and between LOC and pIPS, were bidirectional, while that between pIPS and dlPFC was unidirectional, all at around 15 Hz.

Gamma-oscillations: All nodes displayed peak power at around 80 Hz, with the highest power at dlPFC [Fig. S7 (1st column)]. The coherence spectra [Fig. S7 (2nd column)] for pIPS and dlPFC show that SI and dlPFC were coherently modulated at around 80 Hz. The 3rd and

4th columns of Fig. S7 show the pairwise Granger causality spectra for a pair of network nodes.

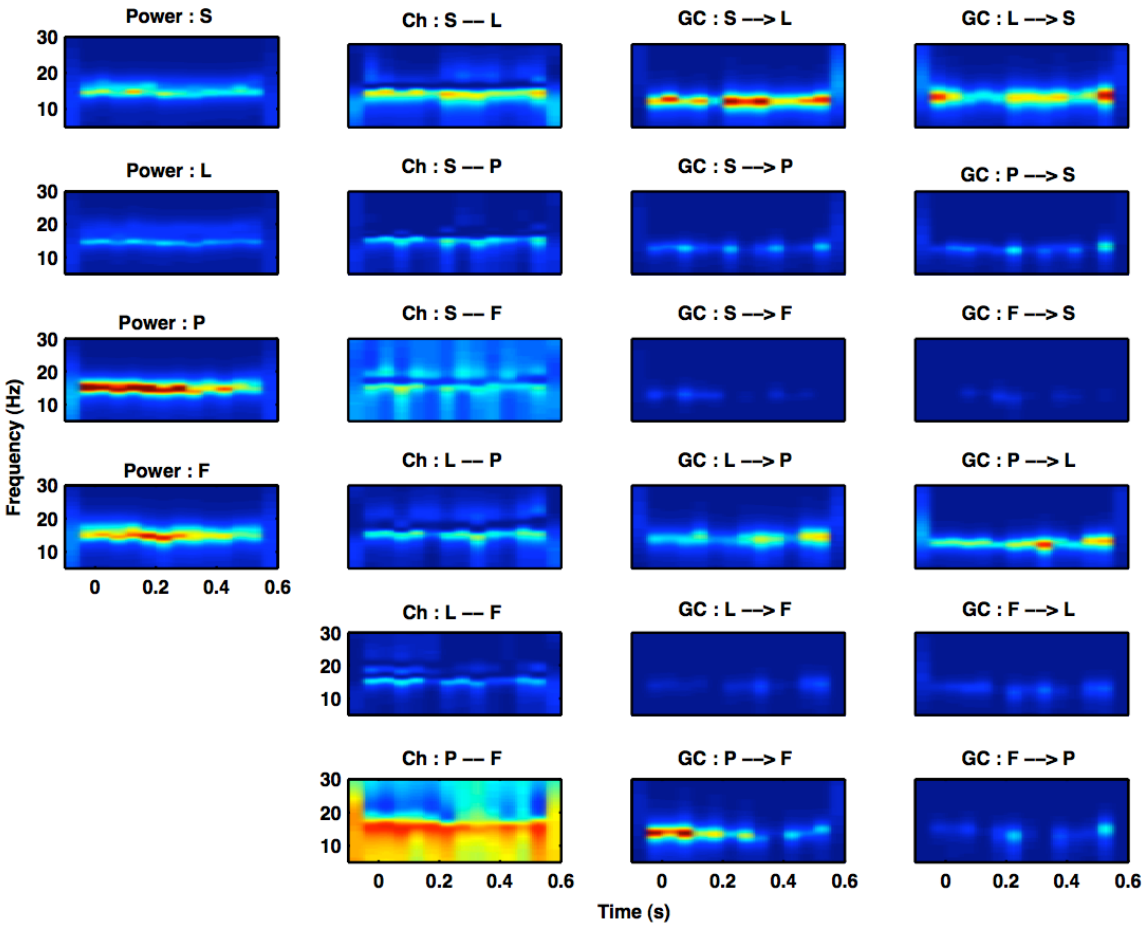

Figure S6*: Time-frequency analysis, beta-oscillations. The first column shows power, the second column shows coherence (Ch), and the third and fourth columns show pairwise Granger causality (GC), where S = SI, L = LOC, P = pIPS, and F = dlPFC. Power, coherence and Granger causality spectra show peaks at around 15 Hz.*

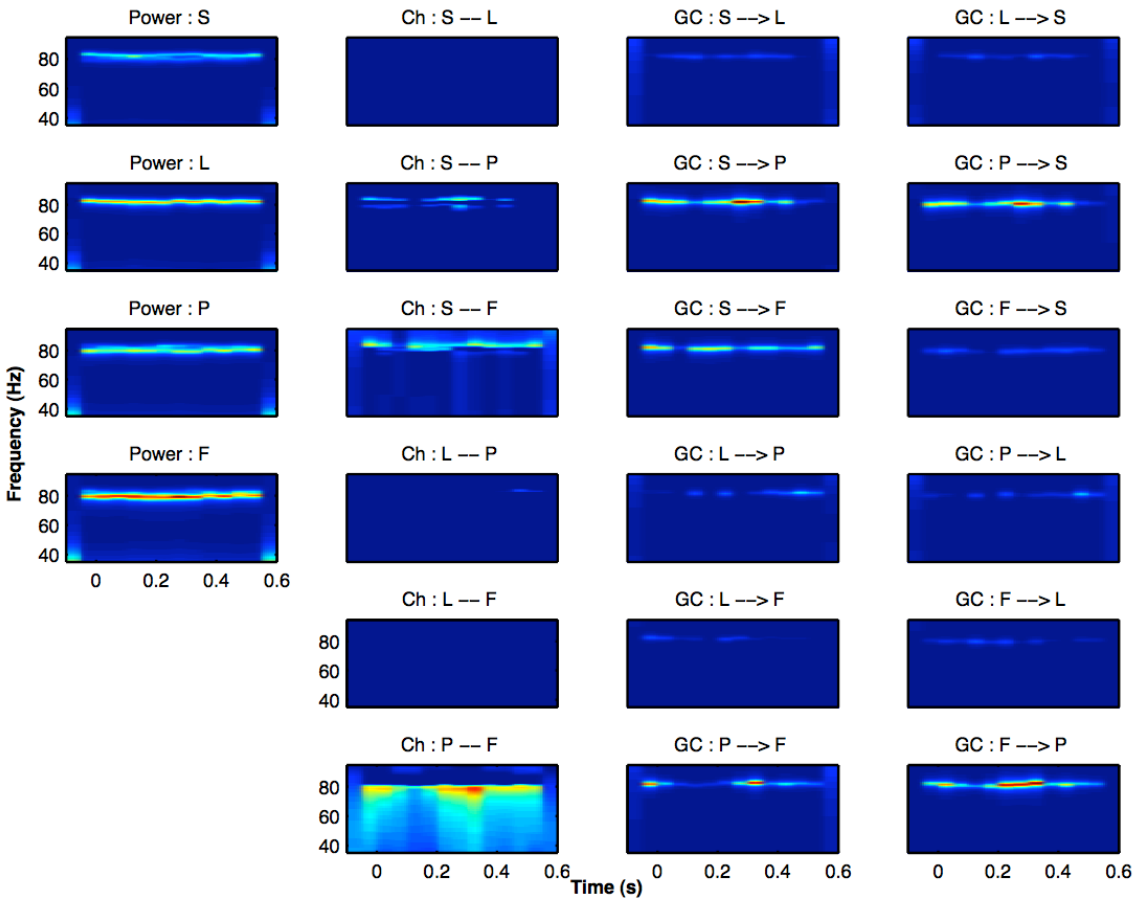

Figure S7*: Time-frequency analysis, gamma-oscillations. The first column shows power (P), the second column, coherence (Ch), and the third and fourth columns, pairwise Granger causality (GC). S, L, P, and F as in Fig. S6. Power, coherence, and Granger causality spectral peaks occur at around 80 Hz.*

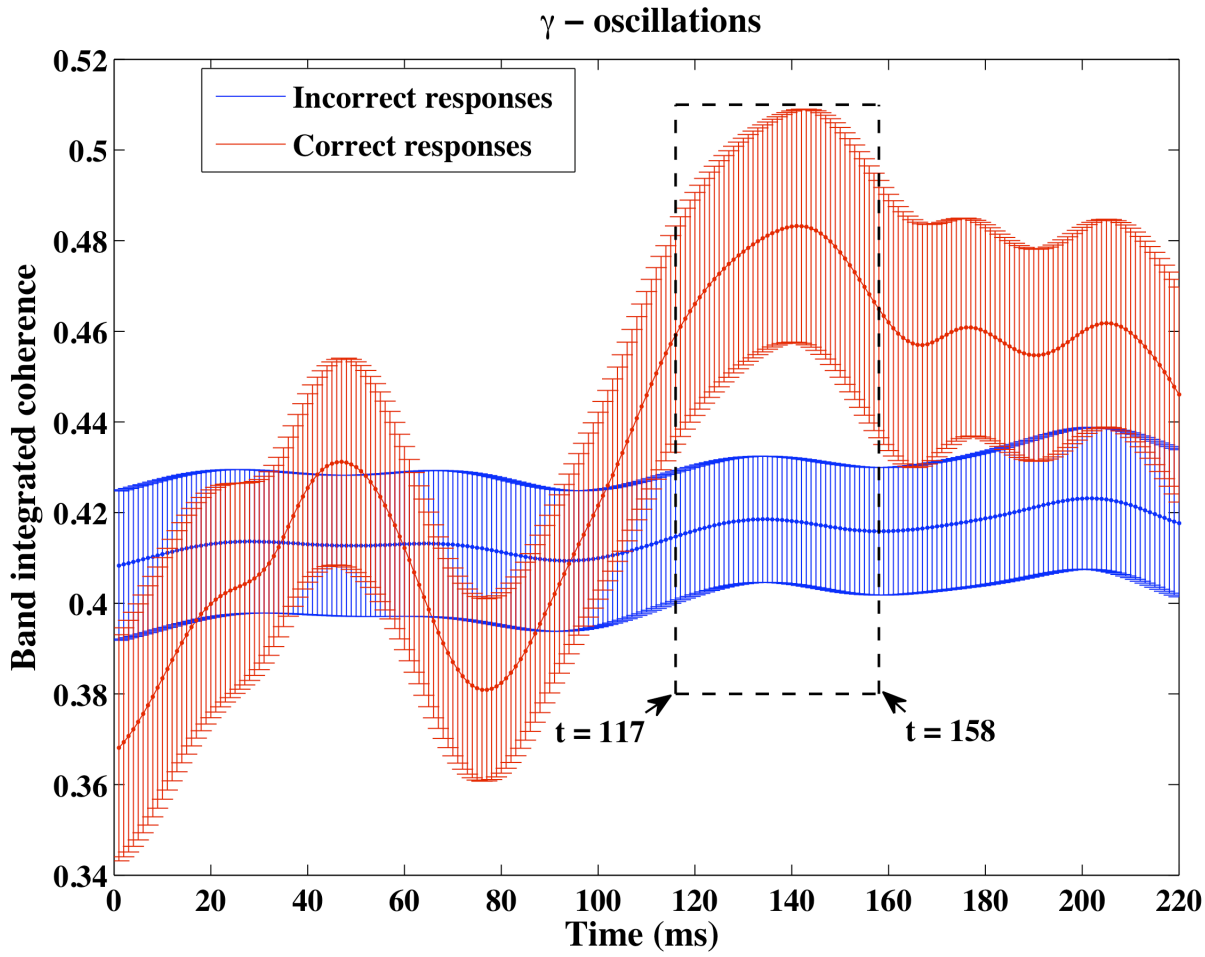

Figure S8*: Gamma coherence (pIPS – dlPFC) during trials with correct and incorrect responses*

VII. Brain-behavior correlation

Here, we include all the results (significant and not significant) trying to establish brain and behavior relationship. We looked at the relationship between the brain and behavior from the task performance accuracy and network activity (coherence and Granger causality). Source waveforms were collected both for correct and incorrect response trials from all network nodes and were used to compute the coherence and the causality spectra across subjects. We computed coherence and Granger causality values separately for both beta and gamma bands from each participant to examine the relationship between behavioral

and electrophysiological data. The coherence values in the beta band (Fig. S9) and gamma band (Fig. S10) are plotted here as a function of average accuracy performance (z-score), for each pair of nodes. We found significant positive correlations between coherence and behavioral performance for SI-LOC and pIPS-dlPFC in the beta band and for pIPS-dlPFC and SI-dlPFC in the gamma band.

Similarly, Fig. S11 and Fig. S12 represent the Granger causal influences as a function of average accuracy in the beta and gamma bands, respectively. In the beta band, the Granger causal influence from pIPS to dlPFC was positively correlated with accuracy whereas the Granger causal influences from SI to LOC and LOC to pIPS tended to be significant. In the gamma band, the Granger causal influences from dlPFC to pIPS and SI to dlPFC were positively correlated with accuracy whereas the Granger causal influences from pIPS to SI tended to be significant.

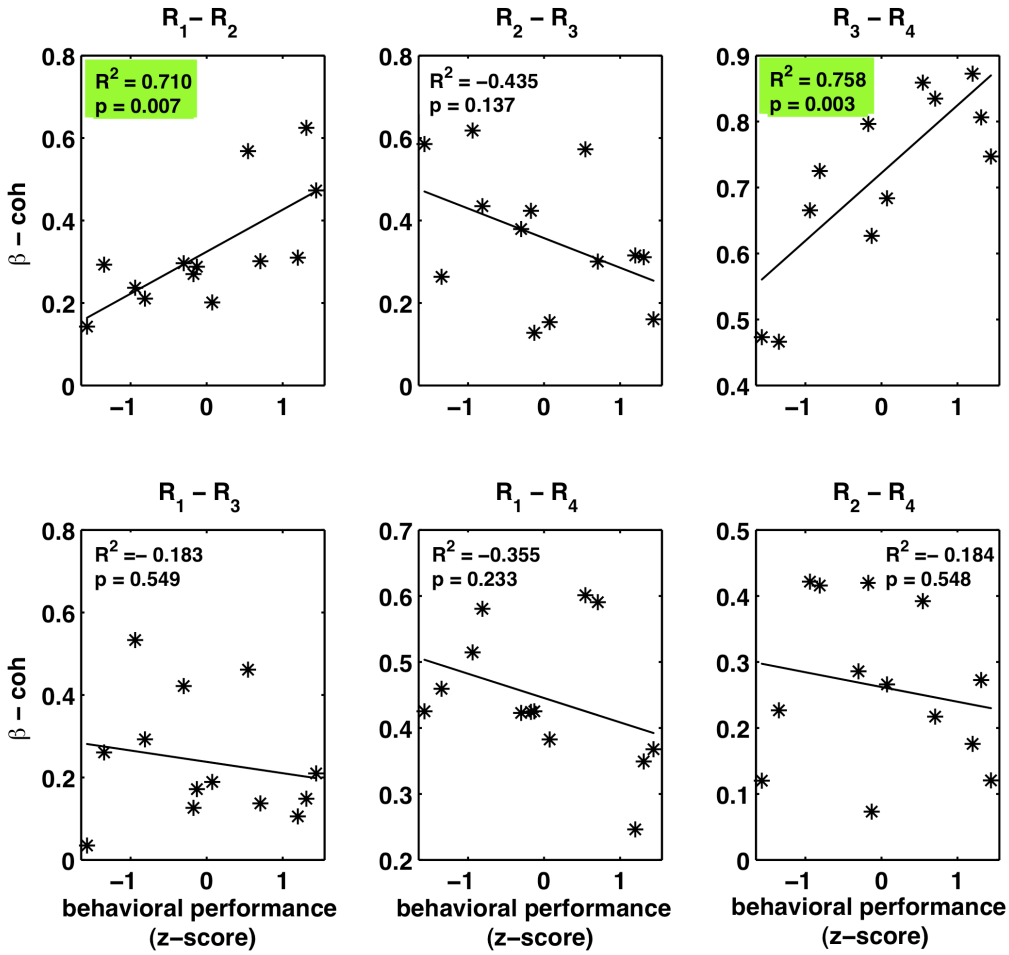

Figure S9*: Relation between coherence and behavioral performance in the beta band. The highlighted subplots show pairs of nodes where coherence was significantly positively correlated with behavioral accuracy (green highlights). R1, R2, R3, and R4 as in Fig. S3.*

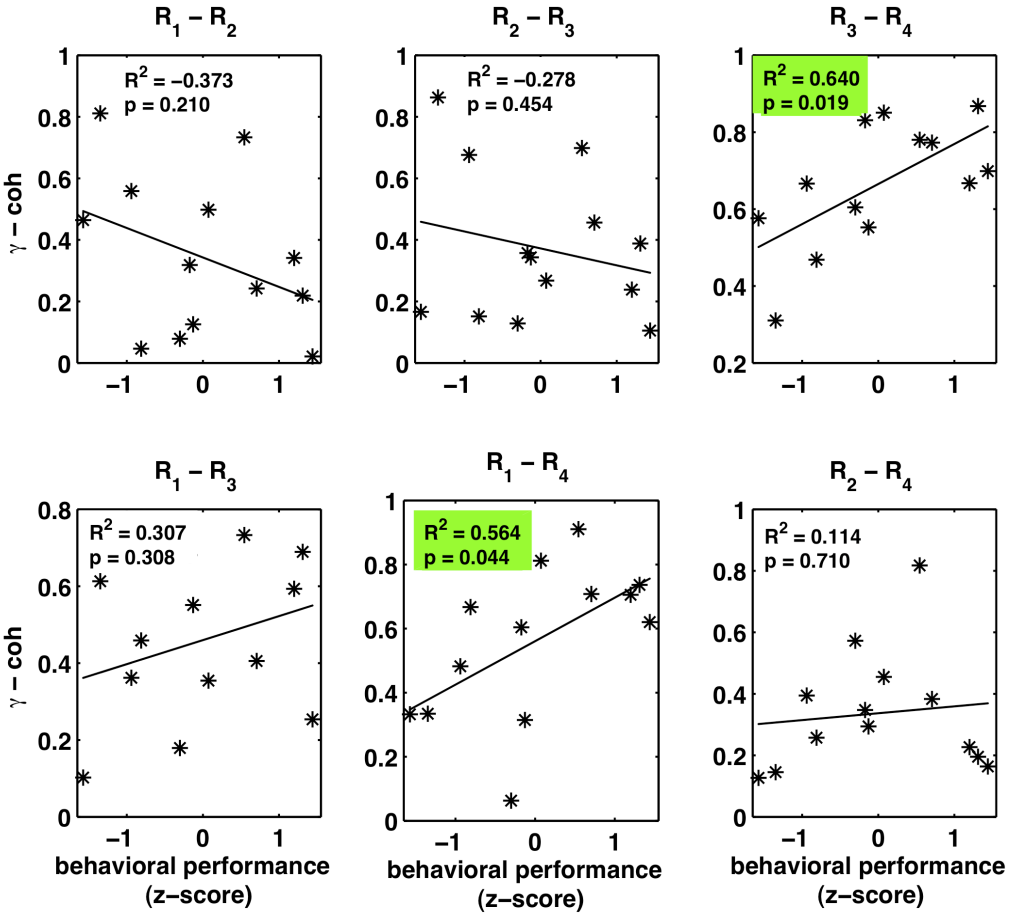

Figure S10: *Relation between coherence and behavioral performance in the gamma band. The subplots highlighted in green represent pairs of nodes with significant positive correlations between coherence and behavioral accuracy. R1, R2, R3, and R4 as in Fig. S3.*

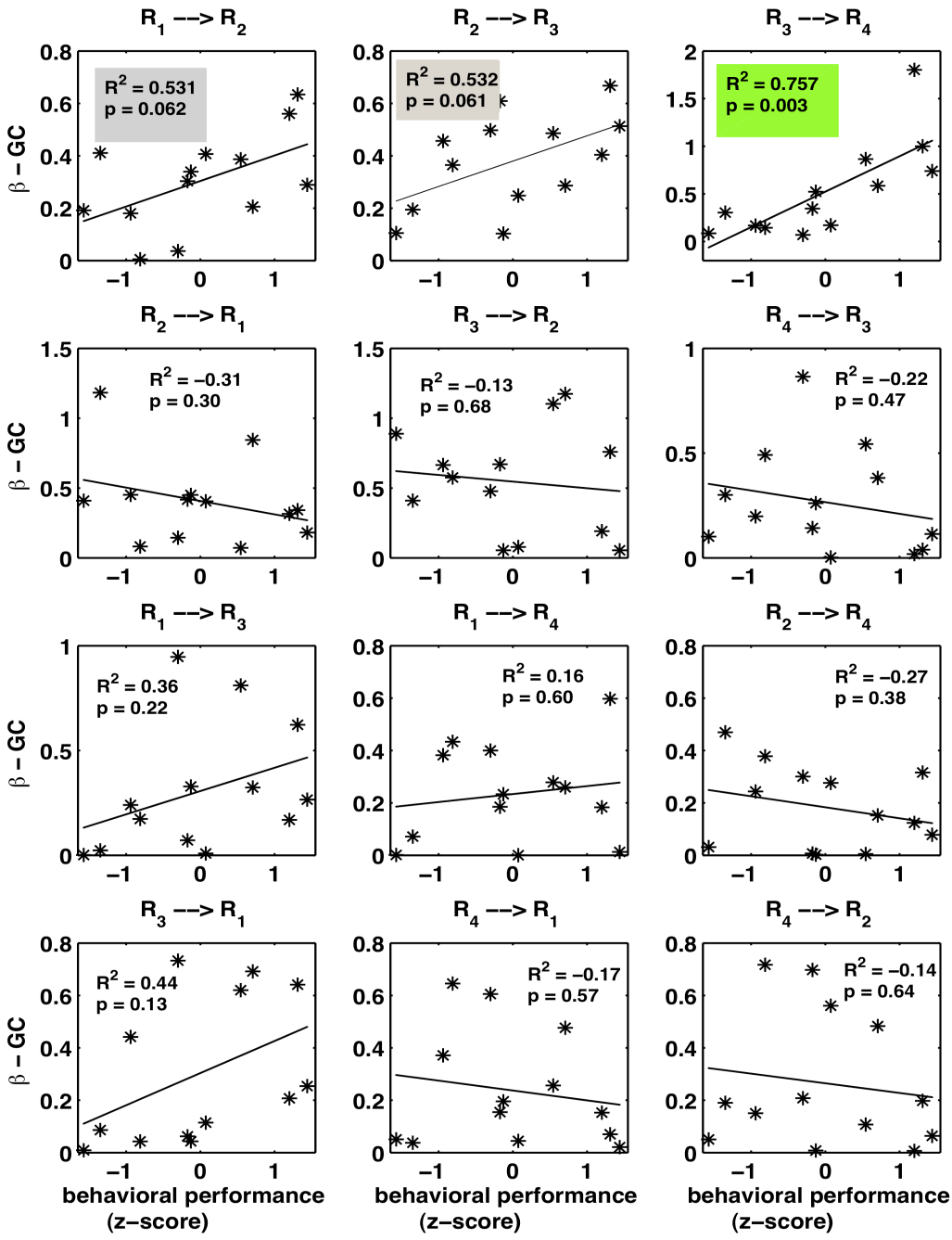

Figure S11: *Relation between Granger causal influences and behavioral performance in the beta band. The highlighted subplots show Granger causal influences significantly positively correlated with behavioral accuracy (green) or tending to be significantly correlated (gray). R1, R2, R3, and R4 as in Fig. S3.*

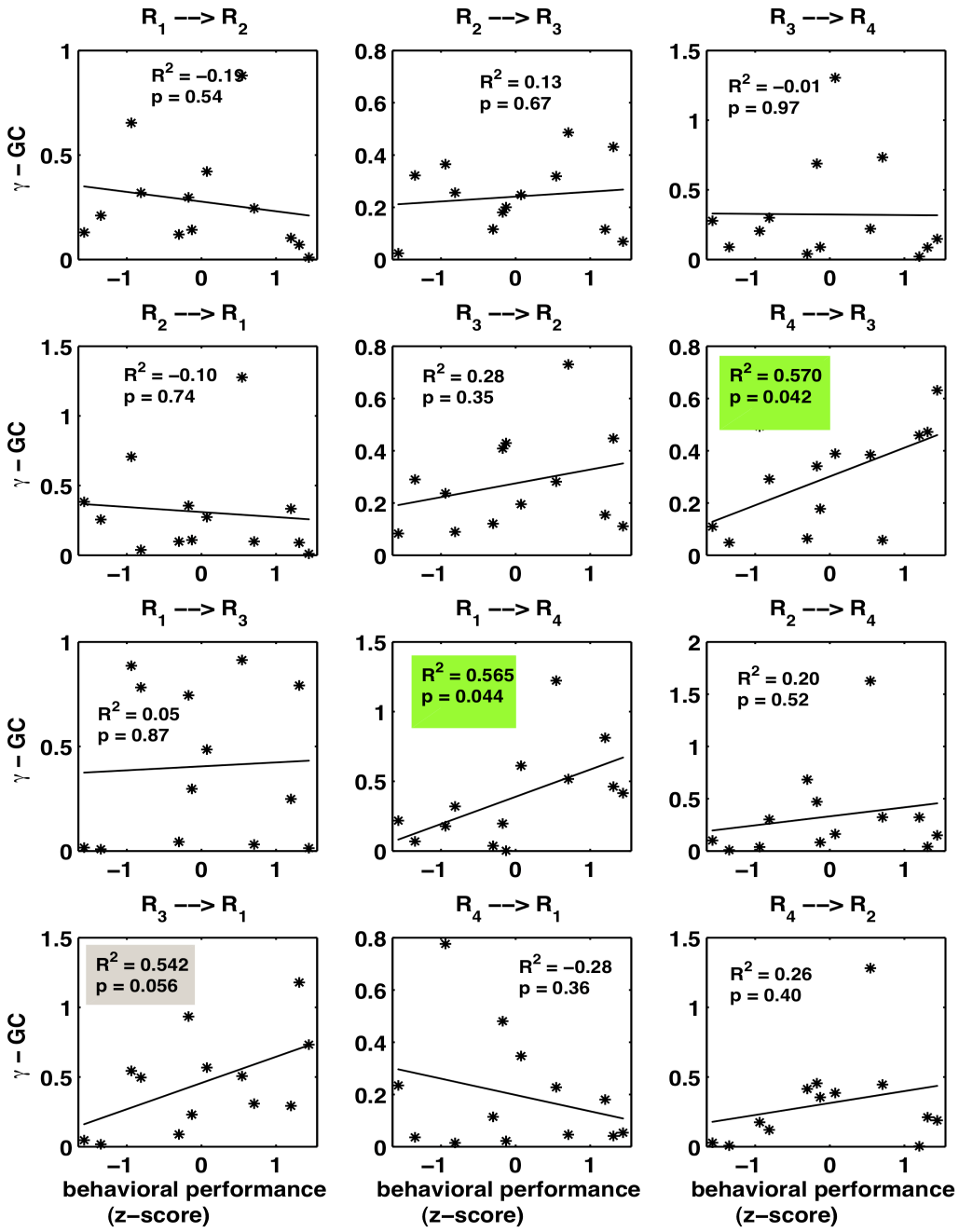

Figure S12: *Relation between Granger causal influences and behavioral performance in the gamma band. The highlighted subplots either show Granger causal influences significantly positively correlated with behavioral accuracy (green) or tending to be significantly correlated (gray color). R1, R2, R3, and R4 as in Fig. S3.*